Georgia Journal of Science

Volume 76 *No.2 Scholarly Contributions from the Membership and Others* | Article 4

2018

Near-Infrared Photometry of Mercury

Richard W. Schmude Jr.
Gordon State College, schmude@gordonstate.edu

Near-Infrared Photometry of Mercury

Acknowledgements
I am grateful to Gordon State College for a Faculty Development Grand which was awarded in 2014 and enabled me to purchase the SSP-4 photometer.

NEAR-INFRARED PHOTOMETRY OF MERCURY

Richard W. Schmude, Jr.
Gordon State College

ABSTRACT

This report summarizes 100 brightness measurements of Mercury made between May 2014 and September 2017 in the J and H near-infrared filters. Brightness models are reported for the J (solar phase angles between 52.3° and 124.5°) and H (solar phase angles between 38.6° and 133.0°) filters. Additional conclusions are as follows: Mercury's brightness is within 0.1 magnitudes, at a given phase angle, for waxing and waning phases, and the geometric albedos at a solar phase angle of 0° are estimated to be 0.16 ± 0.03 and 0.24 ± 0.05 for the J and H filters, respectively.

***Keywords*:** Mercury, J and H filters, photometry

INTRODUCTION

One is able to measure the brightness of a planet by comparing it to one or more stars of known brightness. This kind of measurement is called planetary photometry. This technique can give astronomers insights into a planet's heat budget, surface, and thermal characteristics. Furthermore, in the case of Mercury, it may give astronomers new insights into the behavior of hot exoplanets. Reflected and emitted light are the two sources of light coming from a planet and their intensity depends on the phase. The phase angle is the angle between the observer and the light source measured from the center of the target. The phase angle describes the phase. The reflected light for planets in our solar system is dominated by solar radiation. The amount of emitted light depends on the planet's temperature and wavelength. In the case of Mercury, the phase also affects the amount of emitted light. This is because the daytime temperature is hottest when the Sun is near zenith and is lowest near the morning terminator (Strom and Sprague 2003, 44). Consequently, at a nearly full phase, an observer on Earth faces the hottest part of Mercury; whereas, at a crescent phase the cooler portions face Earth. Therefore, the phase will affect the amount of emitted light.

Harris (1961) reviewed the early photometric measurements of Mercury. He reported that the brightness ratio of light with a wavelength of 2 μm to that with a wavelength of 1 μm light was 3.5. He attributed this high value to "planetary radiation". Veverka et al. (1988) reviewed both photometric and polarimetric measurements made in the wavelength range of 0.3 to 1.1 μm. They report Mercury has a wider range of albedos than the Moon at the scale imaged by Mariner 10. They also report the brightness ratio of the Terrae to Maria is only 1.4 for Mercury compared to 2 for the Moon. Vilas (1988) reviewed spectra made through the mid-1980s. This individual reported that the thermal emission starts to become significant at a wavelength of 1.6 μm. An early spectrum, which includes wavelengths greater than 1.1 μm, was reported by McCord and Clark (1979). These two report a spectrum made between 0.65 μm and 2.5 μm. The intensity increases with increasing wavelength. They report spectra with and without thermal emission. These groups were unable to report how their results changed with the phase angle.

Mallama et al. (2002) used both SOHO (the large angle spectrometric coronagraph instrument on the solar and heliospheric observatory) images and CCD images to

measure the V-filter (wavelength ~0.54 μm) brightness of Mercury at solar phase angles between 2° and 170°. They report a polynomial equation which describes the V filter brightness over the phase angles examined. A geometric albedo of 0.142 ± 0.005 is also reported. This was an important study since it covered a wide range of phase angles. Warell and Bergfors (2008) used a CCD camera to measure the brightness of Mercury in the UBVRI system. Their measurements cover solar phase angles between 22° and 152°. They report Mercury has phase reddening based on the color index measurements. This was an excellent study but there is significant scatter in the data. Schmude (2017) reported preliminary values of the normalized magnitudes of Mercury for a solar phase angle of 60°.

Vernazza et al. (2010) reported a spectrum of Mercury covering the wavelength range 0.9 to 2.4 μm. It was made on February 29, 2008. They illustrated the contribution from both reflected light and from thermal emission. Based on this, the thermal emission is less than 1% for the J filter and is 6% for the H filter. On that date Mercury's solar phase angle was 87° and its distance from the Sun was 0.45 au according to the website https://ssd.jpl.nasa.gov/horizons.cgi. The amount of thermal emission will increase as its sun distance or solar phase angle decreases. On February 29, 2008, the thermal contribution to Mercury's brightness was about equal to reflected light at a wavelength of 2.3 μm (Vernazza et al. 2010). At wavelengths below this value, reflected light contributed more whereas the reverse was true at wavelengths greater than 2.3 μm. This is based on measurements made over a portion of Mercury.

The goals of this study are to 1) report the first J and H filter brightness measurements of Mercury and corresponding brightness models; 2) determine if the brightness depends on the waxing or waning phase and 3) estimate the normalized magnitude at a solar phase angle of zero degrees.

METHOD & MATERIALS

An SSP-4 photometer along with filters transformed to the J and H system were used in recording all brightness measurements. The filter and photometer characteristics are summarized in Table I. A 0.09 m Maksutov telescope was also used. A brightness measurement requires a star of known and nearly constant brightness. Essentially, one records the brightness of a comparison star of known brightness and then measures the brightness of the target. All measurements were made on the stellar magnitude scale. A stellar magnitude corresponds to a specific quantity of electromagnetic radiation. The lower the magnitude value of an object, the brighter it is.

Table I. Summary of filters and the SSP-4 photometer

Item	Description
J filter	Wavelength range = 1.15–1.35 μm[a]
H filter	Wavelength range = 1.5–1.8 μm[a]
SSP-4 photometer detector	Model G5851 by Hamamatsu Corporation[a]
Spectral range of the detector	0.9–2.05 μm[a]
Normal operating temperature	-25 °C[a]
Aperture size	1.0 mm
Field of view (with the 0.09 m Maksutov)	0.11 degrees[b]

[a]Optec, Inc. (2005) [b]Optec, Inc. (1997)

Since different telescopes and detectors have different sensitivities to near-infrared light, a calibration routine is required. In photometry, transformation corrections are this calibration. Transformation coefficients were measured using the star-pair method (Hall and Genet 1988) except J – H replaced B – V. The values for the transformation coefficients for 2014 and 2015 are reported elsewhere (Schmude 2016a). Values for 2016–2017 are $\varepsilon_J = 0.057$ and $\varepsilon_H = 0.006$.

The Earth's atmosphere absorbs near-infrared light. The lower an object is (the closer to the horizon) the more air light must travel through. The absorption of light by the atmosphere is called extinction. Therefore, if the comparison object is at a different elevation above the horizon compared to the target, an extinction correction should be made. Extinction corrections are crucial for accurate Mercury measurements. In all cases measurements were made when the Sun was below the horizon and, hence, Mercury was at low elevations. Fortunately, the atmosphere is more transparent in the infrared than at visible wavelengths. The mean extinction coefficients (April 2014 to November 2017) in magnitudes/air mass, at my observing location (Barnesville, Georgia, elevation ~250 m) are 0.088 and 0.066 for the J and H filters, respectively. The respective standard deviations are 0.043 and 0.036 magnitudes/air mass. The extinction coefficients are much lower than the corresponding values for the V filter, 0.23 magnitudes/air mass (Schmude 2016b). Extinction coefficients were measured for each day Mercury measurements were made. Essentially the brightness of Mercury was measured as its altitude changed. The change in magnitude was plotted versus the air mass and then fitted to a linear equation. The slope was the extinction coefficient. In all cases, the air mass of Mercury was determined from the procedure described in Kasten and Young (1989).

Comparison star magnitudes were taken from Henden (2002). His list contains mostly bright stars. He reports extinction coefficients of 0.10 and 0.06 magnitude/air mass for the J and H filters, respectively. These are close to the author's values.

RESULTS

The measured J and H filter magnitudes, corrected for atmospheric extinction and transformation, are listed in Table II. The J and H magnitudes were normalized as

$$J(1, \alpha) = J_m - 5 \log[r \Delta] \quad (1)$$

$$H(1, \alpha) = H_m - 5 \log[r \Delta] \quad (2).$$

In these equations, J_m and H_m are the J and H filter magnitudes, r is the Mercury-Sun distance in au, Δ is the Mercury-Earth distance in au and $J(1, \alpha)$ and $H(1, \alpha)$ are the normalized magnitudes at a solar phase angle α. The solar phase angle is the angle between the observer and the Sun measured from the target; for Mercury, this ranges from 0° to 180°.

The values of $J(1, \alpha)$ and $H(1, \alpha)$ were plotted against α and the results are shown in Figure 1. The same procedure for Saturn (Schmude 2016a) was carried out for Mercury. Essentially, the normalized magnitudes were fit to six different equations described in Table III and the results are shown in Table IV. Equations 5 and 6 in Table III are based on the relationships

$$J(1, \alpha)' = J_m - 5 \log[r \Delta] + 2.5 \log[(\text{Cosine}(\alpha) + 1)/2] \quad (3)$$

$$H(1, \alpha)' = H_m - 5 \log[r \Delta] + 2.5 \log[(\text{Cosine}(\alpha) + 1)/2] \quad (4)$$

where J(1, α)′ and H(1, α)′ are normalized magnitudes with a geometric correction for the phase and the other symbols are the same as those in equations 1 and 2.

Table II. Brightness measurements of Mercury

Date (filter)	Measured Magnitude	Date (filter)	Measured Magnitude	Date (filter)	Measured Magnitude
2014		2015		2016	
May 24.057 (H)	–2.02	Oct. 23.461 (J)	–2.54	Sept. 30.445 (J)	-2.42
2015		Dec. 18.969 (H)	–3.04[a]	Sep. 30.453 (J)	-2.39
Jan. 18.988 (J)	–1.91	Dec. 19.968 (H)	–3.13[b]	Oct. 1.442 (J)	-2.47
Apr. 30.034 (J)	–2.13	Dec. 25.964 (H)	–3.02	Oct. 1.447 (H)	-3.22
Apr. 30.045(H)	–3.11	Dec. 25.972 (J)	–2.34	Oct. 1.454 (H)	-3.22
May 1.037 (J)	–1.99	2016		Oct. 5.448 (J)	-2.64
May 1.048 (H)	–2.85	Jan. 29.477 (H)	–2.30	Oct. 5.456 (H)	-3.40
May 2.037 (H)	–2.73	Jan. 29.489 (J)	–1.74	Oct. 10.458 (H)	-3.54
May 2.049 (J)	–2.11	Jan. 30.480 (H)	–2.32	Dec. 1.961 (H)	-2.84
May 5.039 (H)	–2.38	Jan. 30.491 (J)	–1.83	Dec. 9.965 (J)	-2.43
May 5.050 (J)	–1.82	Feb. 5.478 (H)	–2.42	Dec. 10.965 (H)	-2.96
May 5.060 (J)	–1.80	Feb. 5.490 (J)	–1.90	Dec. 10.975 (J)	-2.33
May 6.037 (J)	–1.73	Feb. 8.482 (H)	–2.44	2017	
May 6.049 (H)	–2.34	Feb. 8.493 (J)	–1.83	Jan. 25.437 (J)	-1.94
May 6.058 (H)	–2.34	Feb. 11.474 (H)	–2.46	Jan. 25.451 (H)	-2.56
May 8.038 (H)	–2.10	Feb. 11.482 (J)	–1.92	Jan. 31.483 (H)	-2.45
May 8.051 (J)	–1.73	Feb. 11.489 (J)	–1.95	Jan. 31.497 (J)	-1.86
May 8.060 (J)	–1.70	Feb. 13.474 (J)	–1.94[b]	Feb. 1.491 (H)	-2.60
May 10.038 (H)	–1.77	Feb. 13.482 (H)	–2.39[b]	Feb. 2.491 (H)	-2.43
May 10.049 (H)	–1.79	Feb. 13.488 (H)	–2.36[b]	Apr. 1.021 (J)	-1.89
May 10.061 (J)	–1.32	Feb. 18.480 (H)	–2.62	Apr. 1.030 (H)	-2.57
Oct. 14.458 (J)	–2.17	Apr. 10.021 (H)	–3.36	Apr. 1.037 (H)	-2.54
Oct. 15.444 (J)	–2.21	Apr. 10.028 (J)	–2.48	Apr. 1.044 (J)	-1.86[c]
Oct. 15.456 (H)	–3.14	Apr. 17.026 (H)	–2.55	Apr. 7.026 (H)	-1.51
Oct. 16.448 (J)	–2.37	Apr. 17.034 (J)	–1.95	Apr. 7.040 (J)	-1.04
Oct. 16.456 (H)	–3.09	Apr. 17.041 (J)	–1.97	Apr. 9.033 (H)	-1.20
Oct. 17.444 (H)	–3.19	Apr. 17.049 (H)	–2.54	Sep. 7.436 (H)	-1.82
Oct. 17.455 (J)	–2.49	Apr. 17.056 (J)	–1.95	Sep. 7.446 (J)	-1.42
Oct. 20.449 (H)	–3.34	Jun. 8.407 (H)	–2.24	Sep. 18.443 (H)	-3.40
Oct. 20.458 (J)	–2.62	Sep. 13.444 (H)	–1.88	Sep. 18.453 (H)	-3.40
Oct. 21.451 (H)	–3.33	Sep. 23.452 (H)	–1.90[b]	Sep. 20.445 (H)	-3.50
Oct. 21.461 (J)	–2.51	Sep. 29.435 (J)	–2.22	Sep. 20.453 (H)	-3.50[c]
Oct. 22.453 (H)	–3.29	Sep. 29.446 (H)	–3.05	Sep. 21.443 (H)	-3.54
Oct. 22.461 (J)	–2.42	Sep. 29.454 (H)	–3.07		
Oct. 23.452 (H)	–3.42	Sep. 30.436 (H)	–3.14		

[a]Star measurement followed by three Mercury measurements and a star measurement
[b]Large scatter in the data
[c]Based on only two measurements

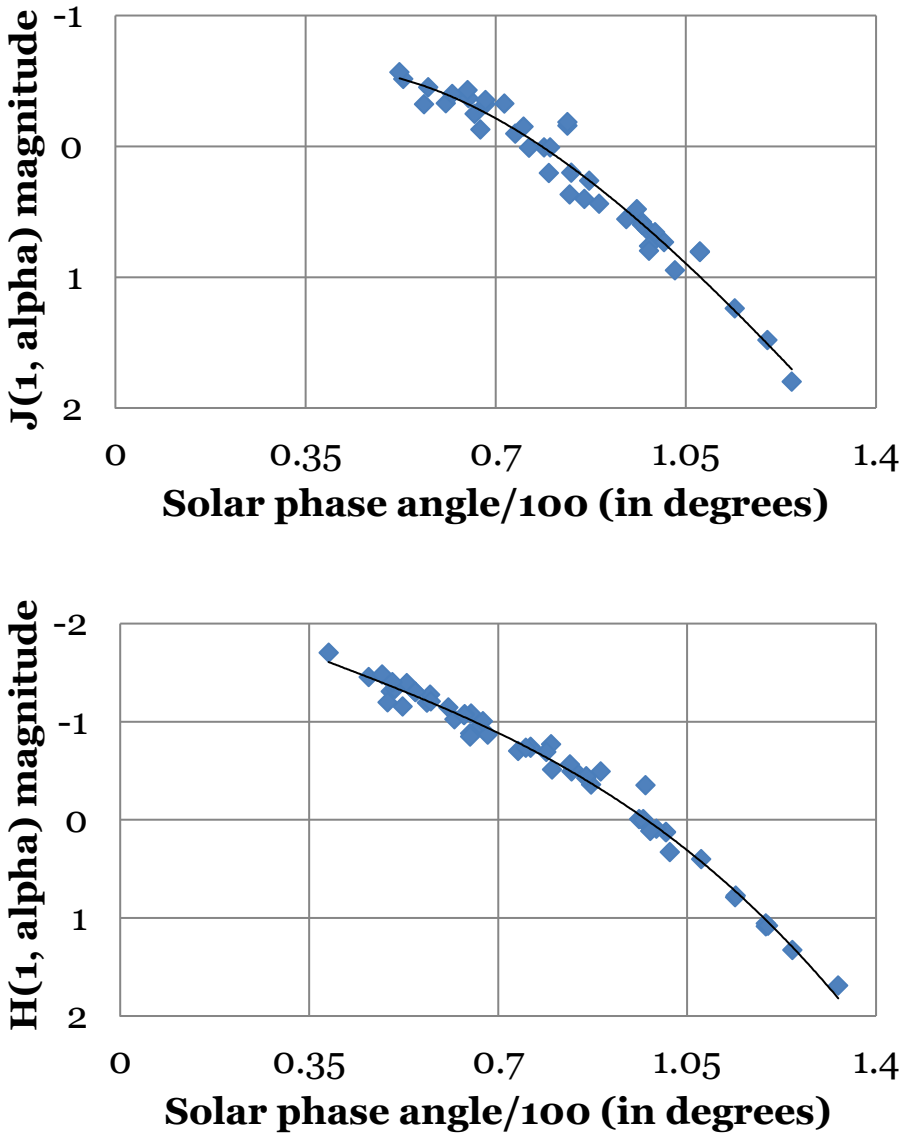

Figure 1. Graphs of J(1, α) and H(1, α) versus the solar phase angle α/100. The curve in both graphs is based on equation 3 in Table IV.

Any of the six models in Table IV could be used over the range of the α values listed. Equation 3 is selected because it has the smallest standard error for the H filter. Mallama et al. (2002) selected a similar polynomial for the V filter measurements.

The standard errors were computed in the usual manner (Larson and Farber 2006). They are larger than those for Saturn (Schmude 2016a). The reason for this is the larger uncertainties from extinction. Mercury was typically measured through several air masses. The uncertainty may be reduced if measurements are made at elevations above 1500 m or made with a digital camera sensitive to the appropriate wavelengths.

DISCUSSION

One of the goals of this study is to determine if Mercury has a brightness difference between waxing and waning phases. Figure 2 illustrates normalized magnitudes for waxing and waning phases. Apparently there are no large brightness changes between these two situations. The J(1, α) values are, on average, 0.05 magnitudes fainter for the waning compared to waxing phases. The corresponding difference for the H filter is 0.03 magnitudes. Therefore, the mean differences are less than 0.1 magnitudes for both filters.

Table III. Descriptions for each of the equations used to fit the J and H brightness data

Equation Number	Description
1	The solar phase angle is negative for waxing phases and positive for waning phases and data are fit to a cubic equation.
2	Same as equation 1 except that data are fit to a quadratic equation.
3	All solar phase angles are positive and data are fit to a cubic equation.
4	All solar phase angles are positive and data are fit to a quadratic equation.
5	A geometric correction factor, 2.5 log[(Cosine(α) +1)/2) is included and data are fit to a linear equation. All α values are positive.
6	Same as equation 5 except that data are fit to a quadratic equation.

Table IV. Brightness models for Mercury. The standard error is abbreviated as SE and is in stellar magnitudes; the range of solar phase angles is given in the second column.

Model	SE (mag.)	J filter Equation ($52.3° < \alpha < 124.5°$)
1	0.12	$J(1,\alpha) = -1.0404 + 0.0471(\alpha/100) + 1.7355(\alpha/100)^2 - 0.0192(\alpha/100)^3$
2	0.12	$J(1,\alpha) = -1.0428 + 0.0303(\alpha/100) + 1.7357(\alpha/100)^2$
3	0.12	$J(1,\alpha) = 0.0871 - 3.7964(\alpha/100) + 5.7279(\alpha/100)^2 - 1.3134(\alpha/100)^3$
4	0.12	$J(1,\alpha) = -0.7129 - 0.8629(\alpha/100) + 2.2715(\alpha/100)^2$
5	0.12	$J(1,\alpha)' = -1.4645 + 1.1998(\alpha/100)$
6	0.12	$J(1,\alpha)' = -1.0603 + 0.2077\,(\alpha/100) + 0.5812(\alpha/100)^2$
Model	**SE (mag.)**	**H filter Equation ($38.6° < \alpha < 133.0°$)**
1	0.094	$H(1,\alpha) = -1.8829 - 0.0163(\alpha/100) + 2.0127(\alpha/100)^2 + 0.0254(\alpha/100)^3$
2	0.094	$H(1,\alpha) = -1.8785 + 0.0076(\alpha/100) + 2.0111(\alpha/100)^2$
3	0.090	$H(1,\alpha) = -2.4722 + 2.6194(\alpha/100) - 1.5756(\alpha/100)^2 + 1.5284(\alpha/100)^3$
4	0.093	$H(1,\alpha) = -1.6606 - 0.5668(\alpha/100) + 2.3493(\alpha/100)^2$
5	0.10	$H(1,\alpha)' = -2.3961 + 1.5635(\alpha/100)$
6	0.092	$H(1,\alpha)' = -1.9676 + 0.4473\,(\alpha/100) + 0.6687(\alpha/100)^2$

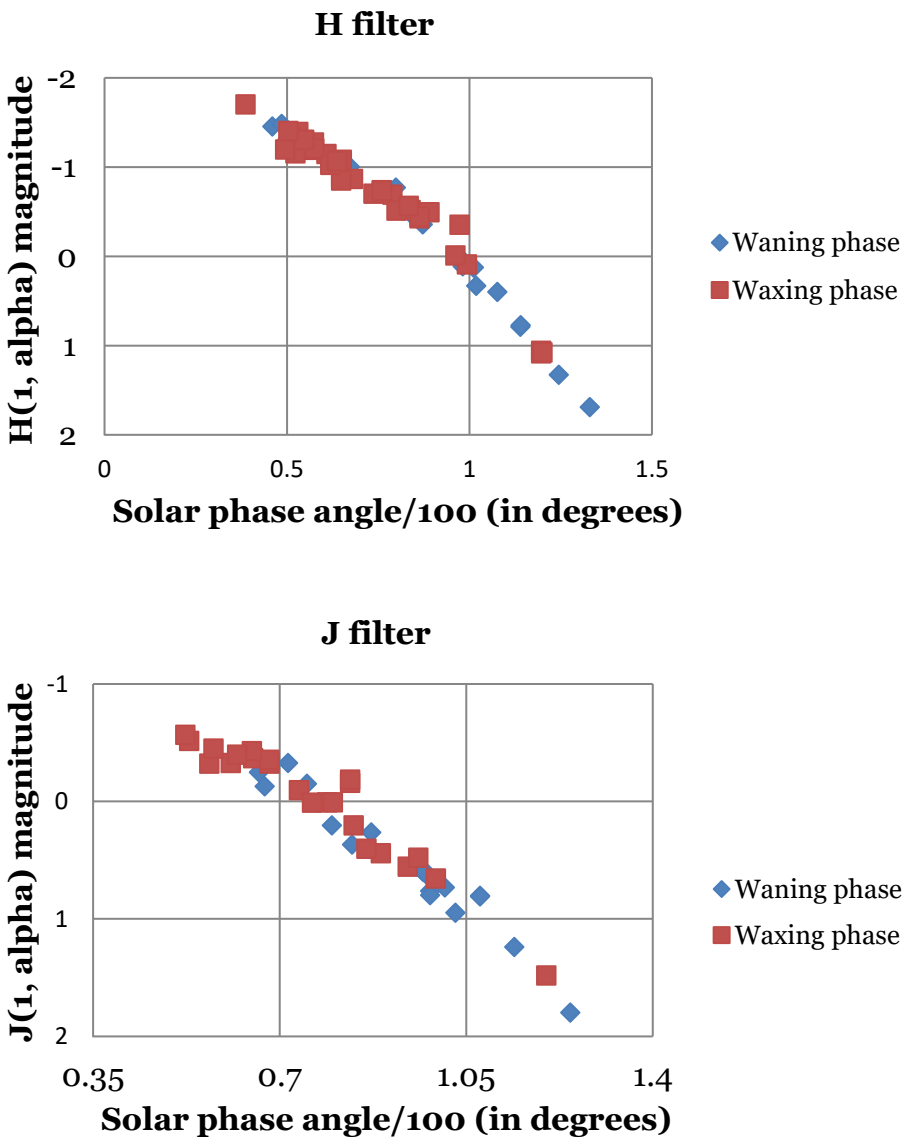

Figure 2. Plots of the J(1, α) and H(1, α) values for waning and waxing phases versus the solar phase angle divided by 100.

Another goal of this study is to estimate the normalized magnitudes of Mercury at a solar phase angle of 0°. This requires extrapolation. The polynomial equations give a wide range of values for α = 0°. Therefore, they should not be used to estimate J(1, 0) and H(1, 0). Instead, equation 5 for both filters is a better option. The author's reason for doing this is that this equation has only one adjustable coefficient and it fits the data almost as well as the others with two or three adjustable coefficients. The extrapolated values are J(1, 0)′ = –1.5 and H(1, 0)′ = –2.4. Mercury grows 0.4 magnitudes brighter as a result of the opposition surge and, hence, this value is subtracted from each extrapolated J or H filter value. Finally, a value of 0.1 magnitudes is added to the H filter value to account for

thermal emission (Vernazza et al. 2010). The selected normalized magnitudes are

$$J(1, 0) = -1.5 - 0.4 = -1.9 \pm 0.2$$
$$H(1, 0) = -2.4 - 0.4 + 0.1 = -2.7 \pm 0.2.$$

With these values along with the J(1, 0) and H(1, 0) values of the Sun (Roddier et al. 2000), the author has computed geometric albedos of 0.16 ± 0.03 and 0.24 ± 0.05 for Mercury based on the procedure in Mallama et al. (2002). These values are higher than those in visible wavelengths and, hence, are consistent with reflectance spectra (Vernazza et al. 2010).

A future goal is to collect more measurements and determine how Mercury brightens at perihelion. Essentially, it receives more than twice the solar energy at perihelion as at aphelion. This will create a larger portion of thermal emission. A second goal is to measure the brightness over a wider range of solar phase angles than what is reported here.

REFERENCES

Hall, D.S. and R.M. Genet. 1988. Photoelectric Photometry of Variable Stars, second revised edition, Willman-Bell, Inc.

Harris, D.L. 1961. Photometry and Colorimetry of Planets and Satellites. *In* Planets and Satellites (G. P. Kuiper and B. M. Middlehurst – editors) University of Chicago Press, 272–342.

Henden, A.A. 2002. JHK Standards for small telescopes. Journal of the American Association of Variable Star Observers, 31, 11–20. http://adsabs.harvard.edu/full/2002JAVSO..31...11H.

Kasten, F. and A.T. Young. 1989. Revised optical air mass tables and approximation formula. Applied Optics, 28(22), 4735–4738. doi:10.1364/AO.28.004735.

Larson, R. and B. Farber. 2006. Elementary Statistics, Pearson Education, Inc.

Mallama, A., D. Wang, and R.A. Howard. 2002. Photometry of Mercury from SOHO/LASCO and Earth: The phase function from 2 to 170°. Icarus, 155, 253–264. doi:10.1006/icar.2001.6723.

McCord, T.B. and R.N. Clark. 1979. The Mercury soil: Presence of Fe^{2+}. Journal of Geophysical Research, 84(B13), 7664–7668.

Optec Inc. 1997. Model SSP-3 Solid-State Stellar Photometer Technical Manual for Theory of Operation and Operating Procedures, Revision 3, Lowell, Michigan, Appendix B.

Optec Inc. 2005. Model SSP-4 Solid-State Infrared Photometer Technical Manual for Theory of Operation and Operating Procedures, Lowell, Michigan.

Roddier, F., C. Roddier, A. Brahic, C. Dumas, J.E. Graves, M.J. Northcott, and T. Owen. 2000. Adaptive optics observations of Saturn's ring plane crossing in August 1995. Icarus, 143, 299–307.

Schmude, R.W. Jr. 2016a. Near-infrared brightness of Saturn. Georgia Journal of Science, 74(2), Article 17. http://digitalcommons.gaacademy.org/gjs/vol74/iss2/17.

Schmude, R.W. Jr. 2016b. Whole-disk brightness measurements of Mars: 2013–2015. Journal of the Association of Lunar and Planetary Observers, 58(2), 42–49.

Schmude, R.W. Jr. 2017. J and H filter photometry of Mercury and the other bright planets. Poster presented at the Lunar and Planetary Science Conference XLVIII. https://www.hou.usra.edu/meetings/lpsc2017/eposter/1578.pdf.

Strom, R.G. and A.L. Sprague. 2003. Exploring Mercury: The Iron Planet. Springer & Praxis Publishing.

Vernazza, P., F. DeMeo, D.A. Nedelcu, M. Birlan, A. Doressoundiram, S. Erard, and E. Volquardsen. 2010. Resolved spectroscopy of Mercury in the near-IR with SpeX/IRTF. Icarus, 209, 125–137. doi:/10.1016/j.icarus.2009.12.010.

Veverka, J., P. Helfenstein, B. Hapke, and J.D. Goguen. 1988. Photometry and Polarimetry of Mercury *in* Mercury (F. Vilas, C. R. Chapman, and M. S. Matthews – editors) University of Arizona Press, 37–58.

Vilas, F. 1988. Surface Composition of Mercury from Reflectance Spectrophotometry *in* Mercury (F. Vilas, C. R. Chapman, and M. S. Matthews – editors) University of Arizona Press, 59–76.

Warell, J. and C. Bergfors. 2008. Mercury's integral phase curve: Phase reddening and wavelength dependence of photometric quantities. Planetary and Space Science, 56, 1939–1948. doi:/10.1016/j.pss.2008.09.002.